Experimental Measurements of Stretching Fields in Fluid Mixing

Greg A. Voth,[1] G. Haller,[2] and J. P. Gollub[1,3,*]

[1]*Department of Physics, Haverford College, Haverford, Pennsylvania 19041*
[2]*Department of Mechanical Engineering, Massachusetts Institute of Technology, Cambridge, Massachusetts 02139*
[3]*Department of Physics, University of Pennsylvania, Philadelphia, Pennsylvania 19104*

(Received 30 November 2001; published 6 June 2002)

Using precision measurements of tracer particle trajectories in a two-dimensional fluid flow producing chaotic mixing, we directly measure the time-dependent stretching field. This quantity, previously available only numerically, attains local maxima along lines that coincide with the stable and unstable manifolds of hyperbolic fixed points of Poincaré maps. Contours of a passive impurity field are found at each instant to be oriented parallel to the lines that have recently experienced large stretching. The local stretching varies by 12 orders of magnitude.

DOI: 10.1103/PhysRevLett.88.254501 PACS numbers: 47.52.+j, 05.45.–a, 47.20.Ky

The mixing of an impurity into a flowing fluid is an important process in many areas of science, including geophysical processes, chemical reactors, and microfluidic devices. Even simple time-periodic flows in two dimensions can produce chaotic mixing and complex distributions of material, in which nearby fluid elements diverge strongly from each other [1]. The fundamental processes involve a combination of repeated stretching and folding of fluid elements in combination with diffusion at small scales. In some cases, for example, periodic flows, the concepts of nonlinear dynamics provide a deep theoretical basis for understanding mixing [2–5]. However, the building blocks of this theory, i.e., the fixed points and invariant manifolds of the associated Poincaré map, have remained inaccessible to direct experimental study, thus limiting the insight that could be obtained.

Computational studies have revealed the importance of both statistical and geometric properties of stretching fields in understanding chaotic mixing [6–11]. Several authors have noted the way a passive scalar pattern is aligned with calculated unstable manifolds of the flow [3,5,12,13]. Recent theoretical work has provided a solid connection between maxima of the stretching field and invariant manifolds of the flow [14,15]. In a flow with an analytically known velocity field, computations of stretching were compared with experimental dye visualization, and the dye was found to have spread over regions that experienced large stretching [12]. In this paper we show that experimental measurements of sufficient accuracy can be used to determine the stretching field for time-periodic flows, thereby revealing the full time-dependent structure of the stable and unstable manifolds of the flow.

To define stretching, consider an infinitesimal circular fluid element. After time Δt, the flow has stretched it into an ellipse, and the amount of stretching is defined as the major diameter divided by its initial diameter. To measure the stretching, we first determine the flow map $\vec{x}' = \vec{\Phi}(\vec{x}, t_0, \Delta t)$, a function that specifies the destination vector $\vec{x}'$ at time $t_0 + \Delta t$ of any fluid particle starting from $\vec{x}$ at time t_0. (For Δt equal to one period, $\vec{\Phi}$ becomes the Poincaré map of the flow.) The stretching experienced by a fluid element is determined by the gradients of the flow map. In particular, the stretching is the square root of the largest eigenvalue of the right Cauchy-Green strain tensor, C_{ij}, at that location: $C_{ij} = (\partial\Phi_k/\partial x_i)(\partial\Phi_k/\partial x_j)$, where summation is implied over the repeated index $k = 1, 2$. Note that the largest finite-time Lyapunov exponent, λ, is given by the logarithm of the stretching after division by Δt.

There are two distinct ways to display the spatial distributions of measured stretching. Labeling each point by the stretching that fluid element will experience in the next Δt produces what we call the future stretching field. The stretching each point experienced in the *previous* Δt is the past stretching field.

Our work depends on high resolution measurements of particle displacements in a two dimensional time-periodic flow described later. Approximately 800 fluorescent latex particles (120 μm in diameter) are suspended in the flow and followed by recording up to 15 000 images (each 512×512 pixels) at 10 Hz in a typical run, or 40–180 images per period. The centroid of each of the 12 000 000 particles in the sequence of images is found to a precision of about 40 μm (0.2 pixels). Particles found in sequential images are then combined into tracks. Since the flow is time periodic, we use conditional sampling, grouping together particle positions in all images at the same phase relative to the forcing. This process yields 100 000 precise particle positions at each phase, velocities accurate to a few percent, spatial resolution of 0.003 of the field of view, and time resolution of about 0.01 periods of the flow.

To extract the flow map and its gradients, we first measure particle velocities from trajectories using polynomial fitting. The velocities are then interpolated onto a grid to obtain the velocity as a function of space and phase. Numerical integration of hypothetical particle trajectories from these velocity fields produces flow maps with extremely high resolution. (We have also used actual particle

trajectories to determine the flow map, and while this produces similar results, it is less accurate.)

The two-dimensional flow is produced by density stratification and time-periodic magnetic forcing [16]. A sinusoidal (horizontal) electric current through a thin conducting fluid layer placed above an array of permanent magnets generates a flow by means of Lorenz forces. The fluid of interest is a 1 mm thick nonconducting upper layer floating on the lower driven layer. The fluids are glycerol-water mixtures, with the lower layer also containing salt. Though miscible, the two layers remain distinct over the course of an experiment, and the flow stays essentially two dimensional. The resulting flow is a time-periodic vortex array, spatially disordered in the work described here. The flow is 15×15 cm, and all the figures in this paper show a central 10×10 cm region. Typical forcing frequencies are 10–200 mHz, and typical velocities are 0.05–1 cm/s. In some experiments, half of the upper layer is initially marked with fluorescein dye, whose emission in the visible under UV illumination is accurately proportional to the local concentration.

The general behavior of this system has been described elsewhere [16]. After an initial transient, the concentration field reaches a nearly steady state in which stretching and folding balance diffusion in such a way that the pattern recurs once per cycle of the forcing (despite the strong variation during the cycle), except for a slow overall exponential decay of contrast. This striking process may be viewed in the animation available on-line [17].

There are two important control parameters. The Reynolds number $\mathrm{Re} = UL/\nu$ (based on the mean magnet spacing $L = 2$ cm, rms velocity U, and kinematic viscosity ν) is typically between 10 and 200. The second parameter is the mean path length $p = UT/L$ in one forcing period T, which is typically in the range 0.5 to 10. Chaotic mixing is weak at the lower end of the ranges of Re and p, where the unmixed elliptic regions are large, and mixing grows stronger as Re and p are increased. Both parameters are controlled experimentally by the forcing current, its frequency, and the fluid viscosity. The flow becomes nonperiodic or weakly turbulent in the range $\mathrm{Re} = 100-150$, depending on p.

Figure 1 shows examples of one component of the velocity field for a run at $\mathrm{Re} = 45$ and $p = 1$. Both components are available as a function of time, and an animation may be viewed on-line [17]. The two fields shown in Fig. 1 are taken at equal time increments before and after the minimum of the magnitude of the velocity field. Because one is not the negative of the other (due to the nonzero Re), particles do not generally retrace their paths and chaotic mixing occurs, despite the periodicity of the flow and the time reversal symmetry of the *forcing*.

Studying mixing requires following fluid elements over extended times. Figure 2 shows the particle displacements over one period, i.e., a Poincaré map. In these maps, lines are drawn from the measured initial to final particle positions, and pseudocolor is used to show the large and small

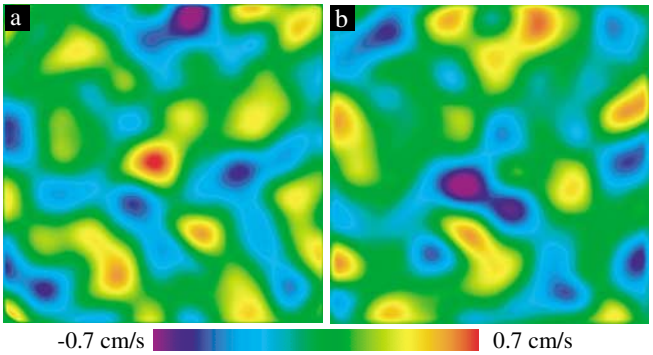

FIG. 1 (color). Maps of one component of the velocity field in the 2D flow measured at two instants equidistant from the instant of minimum flow ($p = 1, \mathrm{Re} = 45$). The fact that one image is not the negative of the other is an example of the breaking of time reversal symmetry required for chaotic mixing.

displacements. Points at which there is no net motion over a full period are fixed points. Figure 2(b) shows a $4\times$ enlargement of part of the Poincaré map. The fixed points in this map have been marked; both elliptic and hyperbolic fixed points may be seen. The latter have one axis of approach (stable manifolds) and one axis of departure (unstable manifolds).

Figure 3(a) shows the past stretching field for this flow. It reveals many sharp maxima which are organized into lines, with much smaller stretching values between them. Determination of the stretching field requires the selection of a time interval Δt for the map; here it is three periods. Smaller (or larger) values result in broader (or sharper) structures. An animation showing how the past stretching field depends on Δt is available on-line [17].

The dye concentration field is shown at the same phase in Fig. 3(b). In Fig. 3(c), we superimpose the past stretching field on the dye image. The dye visualization and particle tracking data are measured in separate experiments at the same parameters. We observe that the level sets (contour lines) of the concentration field line up with the lines

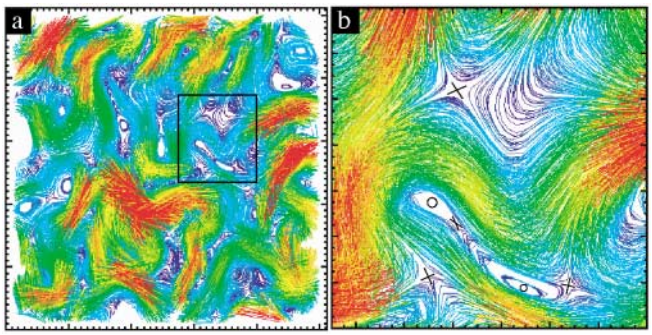

FIG. 2 (color). Poincaré map of the flow at one phase of the forcing ($p = 1, \mathrm{Re} = 45$). Lines connect the experimentally measured initial coordinates of each particle with its coordinates one period later, with blue and red designating small and large displacements, respectively. (a) Complete field of view. (b) Close-up of the region in the box in (a), showing two elliptic fixed points (circles), four hyperbolic fixed points (crosses), and the trajectories near them.

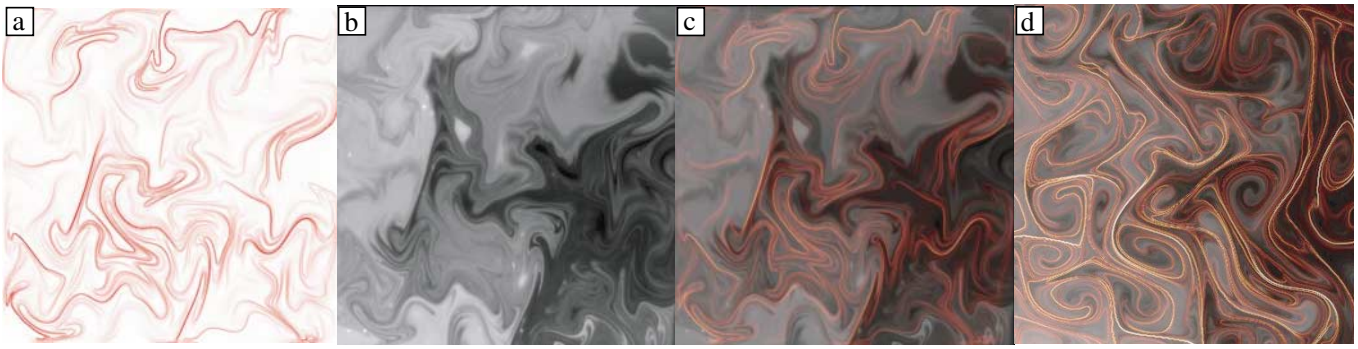

FIG. 3 (color). (a) Field showing the stretching experienced during the past three periods at Re = 45, and $p = 1$. This is the same flow at the same phase as Fig. 2. (b) Corresponding dye image showing the concentration after 30 periods but at the same phase as in (a). (c) Superposition of (a) and (b); the contour lines of the concentration field are aligned with the lines of large past stretching. (d) Superposition of the past stretching field with a dye image at a higher Re = 100 and $p = 5$.

of strong past stretching. Furthermore, we find this to be the case at each instant or phase [17].

Now we discuss the correspondence between the lines of the stretching fields and the fixed points of the Poincaré map. In Fig. 4, we show the future stretching field (blue) in addition to the past stretching field (red). Many of the points where the two sets of lines cross correspond to hyperbolic fixed points of the Poincaré map (Fig. 2b). The lines of the future and past stretching fields label the stable and unstable manifolds of these fixed points [15]. Qualitatively, this is because particles along these manifolds

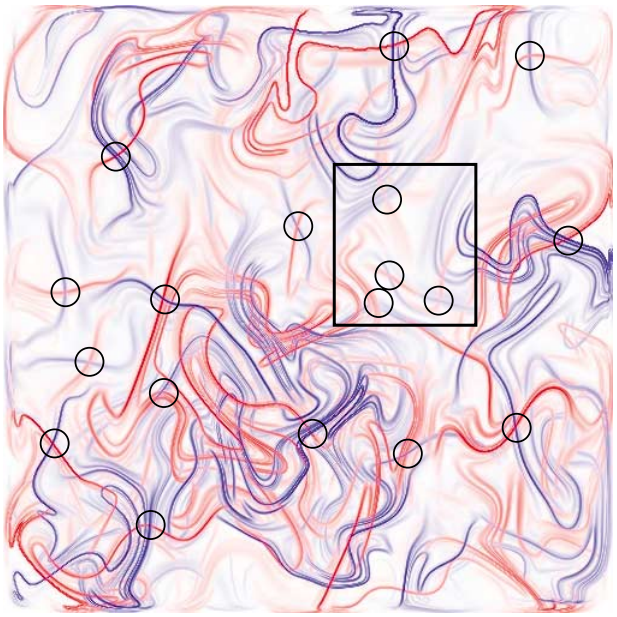

FIG. 4 (color). Lines of the future (blue) and past (red) stretching field. The lines mark the stable (blue) and unstable (red) manifolds of the hyperbolic fixed points of the Poincaré map. Black circles indicate some of the hyperbolic fixed points. Conditions match Figs. 2 and 3(a)–3(c), and the box outlines the region shown in Fig. 2(b). Some of the fixed points are associated with weak stretching lines. Viewing the time dependence of the manifolds [17] allows greater insight into the dynamics of the mixing process.

come very close to a fixed point, and hence experience stretching in the same direction over extended times. Thus, we have the following correspondence between the various objects: large future stretching marks the stable manifolds; large past stretching marks the unstable manifolds. This demonstrated ability to measure the locations of both the stable and unstable manifolds as a function of time in complicated experimental flows allows the insights of lobe dynamics [3,4] to be applied to practical mixing flows. An animation [17] shows the time dependence of the superimposed past and future stretching fields, which form homoclinic and heteroclinic tangles of invariant manifolds. Careful study of this animation makes it possible to distinguish between crossings which mark fixed points and those which do not, since only the former return to their initial location one period later.

We have also carried out this analysis at higher values of Re and p, as shown in Fig. 3(d). Here the fixed points themselves are harder to determine, because much larger stretching is occurring. No regular islands are observed. However, the concentration field is still organized by the invariant manifolds, with contours of constant concentration aligning with the lines of large past stretching. This is particularly dramatic in a time-dependent animation [17].

As Re is increased, the flow passes through a sequence of period doubling bifurcations. At Re = 115, $p = 5$, where Re is only slightly higher than in Fig. 3(d), the velocity field repeats only every second forcing period. At Re = 125, $p = 5$ we find a period-4 velocity field. Despite the bifurcations in the velocity field, the stretching fields measured in the period-2 flow still form sharp lines and the past stretching lines continue to align with the dye pattern at each instant. Although our measurements cannot at present be performed in nonperiodic flows, we note that manifolds that organize the mixing process can be defined and numerically observed even in nonperiodic finite-time flows [14]. This fact suggests that the role the stretching field plays in mixing should be independent of periodicity.

The probability distribution of stretching shown in Fig. 5 displays the wide range of stretching in the flow.

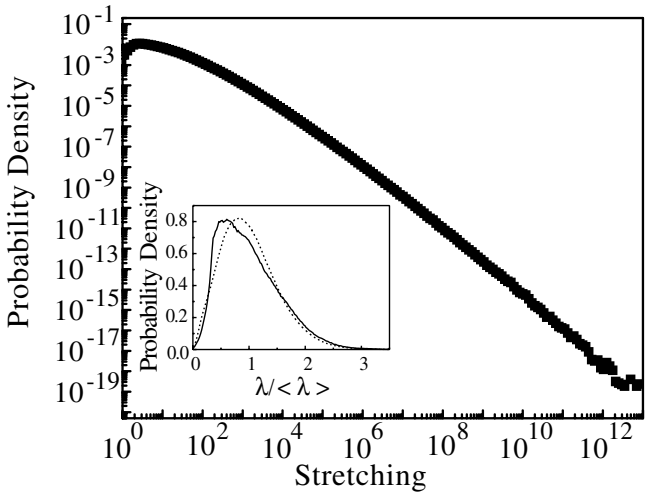

FIG. 5. Probability distribution of stretching for $\Delta t = 1$ period at Re = 100 and $p = 5$. (Inset) Probability distributions of the finite-time Lyapunov exponents, λ. Solid line, Re = 45, $p = 1$, $\langle\lambda\rangle = 1.91$ periods^{-1}; dashed line, Re = 100, $p = 5$, $\langle\lambda\rangle = 6.37$ periods^{-1}.

The log-log plot (at Re = 100, $p = 5$) spans more than 12 orders of magnitude in stretching after only one period. The inset of Fig. 6 shows the distributions of finite time Lyapunov exponents for both the Re = 45 and Re = 100 data. They have been divided by their means, so that the shapes of the distributions can be compared; they depend slightly on Re.

A possible future research direction would be to develop predictions of mixing rates from measured stretching distributions. Theories have been proposed for this purpose [18,19], and have been tested numerically. However, it is uncertain how to apply them to flows like ours that contain regular regions near no-slip boundaries, or whose velocity correlation length is much smaller than the flow domain (due here to the large number of magnets). These issues are treated in a companion paper [20].

We have shown that lines of large stretching corresponding to invariant manifolds of experimental flows can be determined from precise measurements of particle trajectories. These special material lines, which emerge from hyperbolic fixed points of the flow map, organize the evolution of inhomogeneous impurities in the flow. We find that the dye contour lines and the lines of maximal past stretching are locally parallel. This is true at each instant in the time-dependent flow, and continues to be the case at higher Reynolds number and even after the velocity field bifurcates. The ability to measure and visualize the time resolved stretching fields gives powerful insight into the geometrical structure that underlies mixing.

We appreciate helpful discussions with T. Antonsen, B. Eckhardt, E. Ott, and I. Mezic. This work was supported by NSF Grant No. DMR-0072203 (G. V. and J. G.), AFOSR Grant No. F49620-00-1-0133 (G. H.), and NSF Grant No. DMS-0102940 (G. H.).

*Email address: jgollub@haverford.edu.

[1] H. Aref, J. Fluid Mech. **143**, 1 (1984).
[2] J. Ottino, *The Kinematics of Mixing, Stretching, and Chaos* (Cambridge University Press, Cambridge, 1989).
[3] V. Rom-Kedar, A. Leonard, and S. Wiggins, J. Fluid Mech. **214**, 347 (1990).
[4] D. Beigie, A. Leonard, and S. Wiggins, Chaos, Solitons, and Fractals **4**, 749 (1994).
[5] M. Giona, A. Adrover, F. Muzzio, S. Cerbelli, and M. Alvarez, Physica (Amsterdam) **132D**, 298 (1999).
[6] F. Muzzio, P. Swanson, and J. Ottino, Phys. Fluids A **3**, 822 (1991).
[7] F. Muzzio, C. Meneveau, P. D. Swanson, and J. Ottino, Phys. Fluids A **4**, 1439 (1992).
[8] R. T. Pierrehumbert and H. Yang, J. Atmos. Sci. **50**, 2462 (1993).
[9] J. von Hardenberg, F. Fraedrich, F. Lunkeit, and A. Provenzale, Chaos **10**, 122 (2000).
[10] G. Boffetta, G. Lacorata, G. Redaelli, and A. Vulpiani, Physica (Amsterdam) **159D**, 58 (2001).
[11] B. Joseph and B. Legras, J. Atmos. Sci. (to be published).
[12] P. D. Swanson and J. M. Ottino, J. Fluid Mech. **213**, 227 (1990).
[13] A. Péntek, T. Tél, and Z. Toroczkai, J. Phys. A **28**, 2191 (1995).
[14] G. Haller and G. Yuan, Physica (Amsterdam) **147D**, 352 (2000).
[15] G. Haller, Physica (Amsterdam) **149D**, 248 (2001); Phys. Fluids **14**, 1851 (2002).
[16] D. Rothstein, E. Henry, and J. P. Gollub, Nature (London) **401**, 770 (1999).
[17] Video animations which reveal the time dependence of the stretching fields are available at (http://www.haverford.edu/physics-astro/gollub/stretchlines/). For archival purposes, they are also available as AIP Document No. EPAPS: E-PRLTAO-88-032223, which can be retrieved from the EPAPS homepage (http://www.aip.org/pubservs/epaps.html).
[18] T. Antonsen, Z. Fan, E. Ott, and E. Garcia-Lopez, Phys. Fluids **8**, 3094–3104 (1996).
[19] A. K. Pattanayak, Physica (Amsterdam) **148D**, 1–19 (2001).
[20] G. A. Voth, G. Dobler, L. Montagnon, T. Saint, and J. Gollub (to be published).